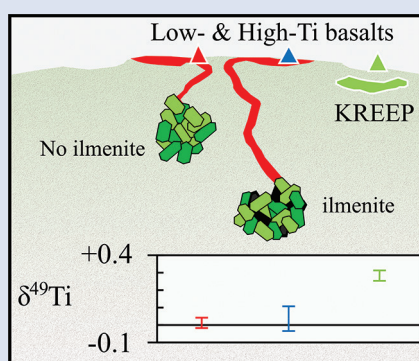# Unravelling lunar mantle source processes *via* the Ti isotope composition of lunar basalts

S. Kommescher[1]*, R.O.C. Fonseca[1,2], F. Kurzweil[1], M.M. Thiemens[1,3], C. Münker[1], P. Sprung[1,4]

Abstract

doi: 10.7185/geochemlet.2007

Formation and crystallisation of the Lunar Magma Ocean (LMO) was one of the most incisive events during the early evolution of the Moon. Lunar Magma Ocean solidification concluded with the coeval formation of K-, REE- and P-rich components (KREEP) and an ilmenite-bearing cumulate (IBC) layer. Gravitational overturn of the lunar mantle generated eruptions of basaltic rocks with variable Ti contents, of which their δ^{49}Ti variations may now reflect variable mixtures of ambient lunar mantle and the IBC. To better understand the processes generating the spectrum of lunar low-Ti and high-Ti basalts and the role of Ti-rich phases such as ilmenite, we determined the mass dependent Ti isotope composition of four KREEP-rich samples, 12 low-Ti, and eight high-Ti mare basalts by using a ^{47}Ti-^{49}Ti double spike. Our data reveal significant variations in δ^{49}Ti for KREEP-rich samples (+0.117 to +0.296 ‰) and intra-group variations in the mare basalts (-0.030 to +0.055 ‰ for low-Ti and +0.009 to +0.115 ‰ for high-Ti basalts). We modelled the δ^{49}Ti of KREEP using previously published HFSE data as well as the δ^{49}Ti evolution during fractional crystallisation of the LMO. Both approaches yield δ^{49}Ti$_{KREEP}$ similar to measured values and are in excellent agreement with previous studies. The involvement of ilmenite in the petrogenesis of the lunar mare basalts is further evaluated by combining our results with element ratios of HFSE, U and Th, revealing that partial melting in an overturned lunar mantle and fractional crystallisation of ilmenite must be the main processes accounting for mass dependent Ti isotope variations in lunar basalts. Based on our results we can also exclude formation of high-Ti basalts by simple assimilation of ilmenite by ascending melts from the depleted lunar mantle. Rather, our data are in accord with melting of these basalts from a hybrid mantle source formed in the aftermath of gravitational lunar mantle overturn, which is in good agreement with previous Fe isotope data.

Introduction

It is widely accepted that the Moon formed as the result of an impact between one or more planetesimals and the proto-Earth (*e.g.,* Asphaug, 2014). The last phases to solidify in the impact-induced Lunar Magma Ocean (LMO) were K-, REE-, and P-rich residual components (urKREEP) and complementarily an ilmenite-bearing cumulate (IBC; Warren and Wasson, 1979; Snyder *et al.,* 1992). Subsequent magmatic processes concluded with the eruption of lunar mare basalts (*e.g.,* Gross and Joy, 2016). Experimental studies and the Hf and Nd isotope composition of mare basalts suggest that low-Ti mare basalts likely result from partial melting of lunar mafic cumulates, whereas high-Ti mare basalts are thought to reflect IBC involvement (*e.g.,* Longhi, 1992; Sprung *et al.,* 2013). However, whether high-Ti basalts result from IBC assimilation by mafic low-Ti magmas (*e.g.,* Münker, 2010), or from the partial melting of a hybridised lunar mantle source (Snyder *et al.,* 1992), remains ambiguous. Titanium isotope variations in mare basalts may be used to discriminate between the two scenarios: refractory, lithophile, and fluid-immobile Ti is predominantly tetravalent albeit lunar samples may contain significant amounts of Ti^{3+} (Simon and Sutton, 2017; Leitzke *et al.,* 2018). The principal Ti-bearing phase in the lunar mantle is ilmenite whose VI fold coordinated crystal site preferentially incorporates lighter over heavier Ti isotopes (Schauble, 2004). The Ti isotope composition of terrestrial samples (given as $\delta(^{49}Ti/^{47}Ti)_{OL-Ti}$, relative to the Origins Lab reference material, henceforth δ^{49}Ti; Millet and Dauphas, 2014) ranges between -0.046 and +1.8 ‰. Observed covariations between δ^{49}Ti and SiO_2, TiO_2, and FeO contents of terrestrial volcanic rocks suggest that stable Ti isotope variation is mainly driven by the onset of fractional crystallisation of Fe-Ti oxides during magmatic differentiation (Millet *et al.,* 2016; Greber *et al.,* 2017a,b; Deng *et al.,* 2018a, 2019; Mandl

1. Institut für Geologie und Mineralogie, Universität zu Köln, Germany
2. Institut für Geologie, Mineralogie und Geophysik, Ruhr-Universität Bochum, Germany
3. G-TIME Laboratory, Université Libre de Bruxelles, Belgium
4. Hot Laboratory Division (AHL), Paul Scherer Institut, Villigen, Switzerland
* Corresponding author (e-mail: s.kommescher@uni-koeln.de)

et al., 2018). Consequently, the Ti isotope composition of lunar magmas might be a sensitive indicator for the crystallisation of the IBC, and its assimilation or partial melting: Millet *et al.* (2016) reported δ^{49}Ti variations in three low-Ti mare basalts with a pooled δ^{49}Ti of -0.008 ± 0.019 ‰ and five high-Ti mare basalts with δ^{49}Ti between +0.011 and +0.033 ‰. The presence of more fractionated δ^{49}Ti in mare basalts, although suggested, has not yet been reported (Millet *et al.*, 2016). Indeed, for the urKREEP end member, as represented by the lunar meteorite Sayh al Uhaymir (SaU) 169, a tentative δ^{49}Ti of +0.330 ± 0.034 ‰ was obtained (Greber *et al.*, 2017b).

Here we report the δ^{49}Ti of 24 representative lunar samples in order to investigate their mantle sources in the context of three major end members: the ambient lunar mantle (low-Ti), the late stage cumulates (IBC, high-Ti), and the residual KREEP-rich component. Notably, the processes that affect δ^{49}Ti in lunar mantle cumulates and corresponding melts also fractionate high field strength element ratios (HFSE; Münker, 2010). High precision HFSE, W, U, and Th data, obtained for the same samples (Thiemens *et al.*, 2019), can help to constrain δ^{49}Ti$_{urKREEP}$, δ^{49}Ti$_{IBC}$ and to identify the processes leading to δ^{49}Ti variations in lunar samples.

Results

Titanium isotope measurements were performed using the Thermo Neptune Plus MC-ICPMS at the University of Cologne with an intermediate precision better than ±0.023 ‰ (2 x standard deviation, henceforth s.d.) for spiked reference materials BCR-2, JB-2, OL-Ti, and Col-Ti. Total blank contribution was always less than 10 ng total Ti and is negligible compared to at least 30 μg of processed sample Ti (20 μg for 68115). More detailed information on the analytical protocol are given in the Supplementary Information. Low-Ti mare basalts show small, resolvable variations in δ^{49}Ti between -0.030 and +0.055 ‰ with an average of +0.010 ± 0.015 ‰ (2 s.d.; n = 12, Fig. 1, Table 1). Most high-Ti samples range from +0.009 to +0.047 in δ^{49}Ti (average of +0.026 ± 0.036 ‰, 2 s.d.; n = 7), sample 75035 has a comparatively high δ^{49}Ti value of +0.115 ‰. The high-Ti average (including 75035) yields a δ^{49}Ti of +0.037 ± 0.071 ‰. KREEP-rich lithologies have δ^{49}Ti values between +0.117 and +0.296 ‰.

Discussion

Estimating the δ^{49}Ti of urKREEP and the IBC. The co-genetic relationship between urKREEP and IBC permits studying the coupled δ^{49}Ti evolution of both reservoirs. Complementarily to the low δ^{49}Ti$_{IBC}$, the residual LMO is expected to have positive δ^{49}Ti (Millet *et al.*, 2016; Greber *et al.*, 2017b). Furthermore, U became enriched in urKREEP, whereas Ti, Hf and Zr are more compatible in ilmenite and are extracted from the LMO during IBC formation. The observed positive co-variation of δ^{49}Ti and U concentration in KREEP-rich samples may therefore indicate variable portions of the urKREEP-component (Fig. 2b). Our KREEP-rich sample with highest δ^{49}Ti and highest U concentration is identical within uncertainty to the previous estimate for δ^{49}Ti$_{urKREEP}$ (Greber *et al.*, 2017b). Two KREEP-rich samples along with SaU169 have U/Hf, U/Zr and U/Ti in the range of the urKREEP estimate (calculated using data by Warren and Taylor, 2014), which results in a conservative estimate of δ^{49}Ti$_{urKREEP}$ of +0.296 ± 0.067 ‰ (see Supplementary Information). To model δ^{49}Ti$_{urKREEP}$ in a different approach, we constrained the evolution of Ti, Hf and Ta concentrations in the remaining liquid during fractional crystallisation for various LMO solidification models (Snyder *et al.*, 1992; Lin *et al.*, 2017; Charlier *et al.*, 2018; Rapp

Table 1 Summary of reference materials and measured samples. For reference materials, n gives the number of sequences in which the material has been measured at least 6 times. Abbreviations are the same as in Figure 1. Two aliquots of OL-Ti were run through the chemical separation process and are given as OL-Ti (chemistry).

			δ^{49}Ti	2 s.d.	n	95 % c.i.
	JB-2		-0.044	0.023	7	0.011
	BCR-2		-0.025	0.012	4	0.010
	OL-Ti mean		0.000	0.001	8	0.000
	OL-Ti (chemistry)		-0.001	0.030	2	0.137
	Col-Ti mean		0.206	0.021	8	0.009
Low-Ti rocks						
12022	Apollo 12	Low-Ti ilm basalt	0.029	0.022	6	0.011
12051	"	Low-Ti ilm basalt	0.030	0.022	8	0.009
12063	"	Low-Ti ilm basalt	0.055	0.022	6	0.012
12054	"	Low-Ti ilm basalt	0.028	0.026	6	0.014
12004	"	Low-Ti olv basalt	0.006	0.010	6	0.005
12053	"	Low-Ti pgt basalt	-0.013	0.026	6	0.014
15495	Apollo 15	Low-Ti ONB	0.011	0.017	6	0.009
15555	"	Low-Ti ONB	-0.008	0.026	6	0.014
15556	"	Low-Ti ONB	0.007	0.030	6	0.016
15065	"	Low-Ti QNB	-0.030	0.014	6	0.007
15058	"	Low-Ti QNB	-0.010	0.034	6	0.018
15545	"	Low-Ti QNB	0.011	0.032	6	0.017
Low-Ti mean ± 2 s.d.			0.010	0.047	12	
High-Ti rocks						
10017	Apollo 11	High-Ti ilm basalt	0.009	0.024	6	0.012
10020	"	High-Ti ilm basalt	0.011	0.022	6	0.011
10057	"	High-Ti ilm basalt	0.009	0.024	6	0.012
74255	Apollo 17	High-Ti ilm basalt	0.043	0.010	6	0.005
74275	"	High-Ti ilm basalt	0.045	0.010	6	0.005
75035	"	High-Ti ilm basalt	0.115	0.025	6	0.013
79135	"	High-Ti bce	0.019	0.017	6	0.009
79035	"	High-Ti bce	0.047	0.018	6	0.010
High-Ti mean 1 ± 2 s.d.			0.026	0.036	7	
High-Ti mean 2 ± 2 s.d.			0.037	0.071	8	
KREEP-rich rocks						
14305	Apollo 14	KREEP-rich bce	0.296	0.030	6	0.016
14310	"	KREEP basalt	0.263	0.035	6	0.018
72275	Apollo 17	KREEP-rich bce	0.185	0.026	6	0.014
68115	Apollo 16	KREEP-rich bce	0.117	0.027	6	0.014

and Draper, 2018) starting with LMO element abundances by Münker (2010) and calculated δ^{49}Ti$_{melt}$ using a Rayleigh distillation model (see Supplementary Information). The intersect of the respective Ti, Hf and Ta concentrations with urKREEP concentration estimates by Warren and Taylor (2014) together with the modelled δ^{49}Ti$_{melt}$-evolution line yield a range for δ^{49}Ti$_{urKREEP}$: all estimates using the above mentioned models and LMO concentrations of Ta (δ^{49}Ti$_{urKREEP}$ = +0.308 ± 0.064 ‰), Hf (δ^{49}Ti$_{urKREEP}$ = +0.290 ± 0.040 ‰) and Ti (δ^{49}Ti$_{urKREEP}$ = +0.238 ± 0.085 ‰) are identical to our KREEP-rich sample with highest δ^{49}Ti (+0.296 ± 0.016 ‰), and previous estimates for δ^{49}Ti$_{urKREEP}$ (Greber *et al.*, 2017b). Our models predict a final δ^{49}Ti$_{IBC}$ between -0.006 and -0.012 ‰, consistent with estimates by Millet *et al.* (2016).
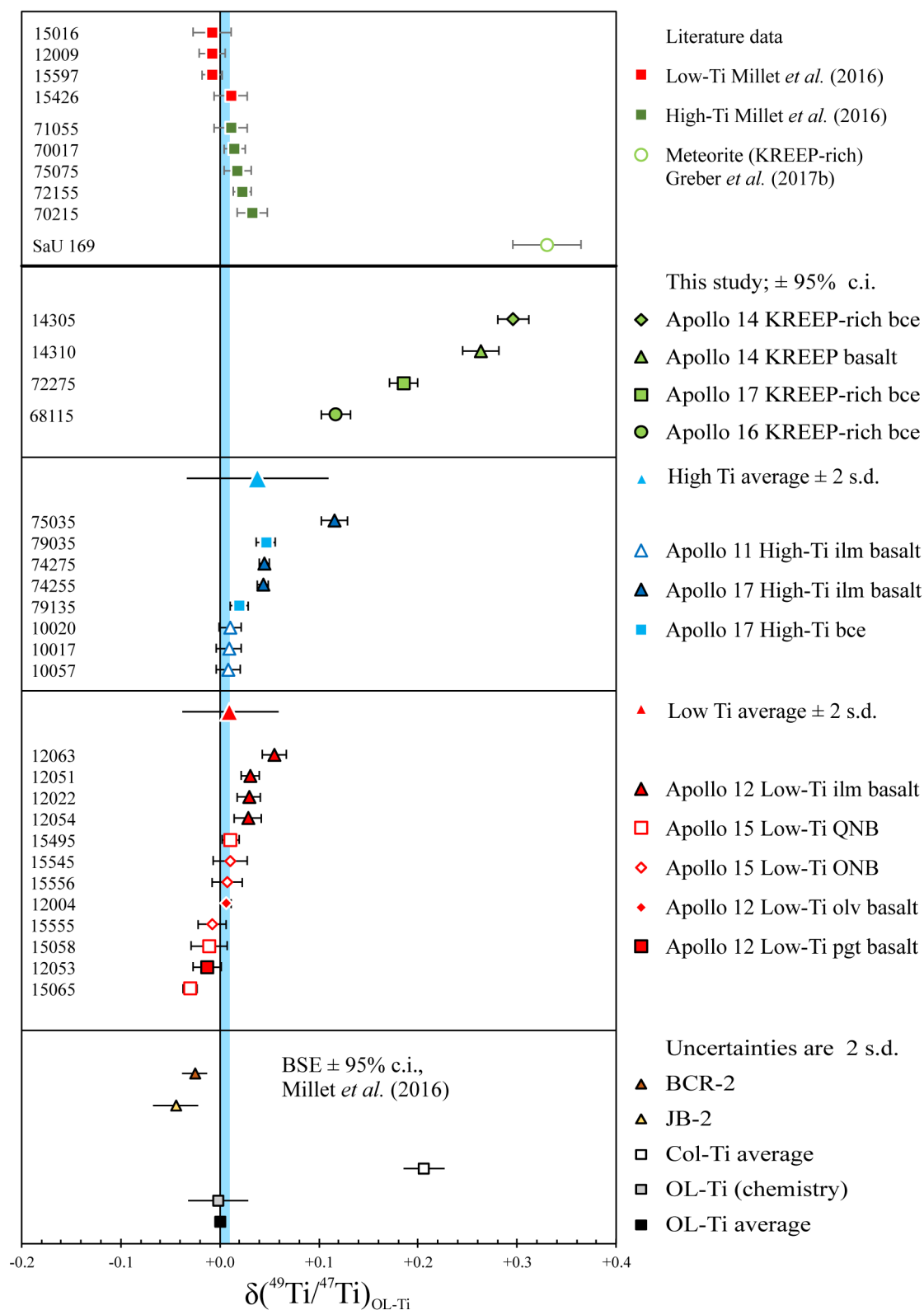
Figure 1 Measured Ti isotope compositions of lunar samples. All uncertainties unless stated otherwise are 95 % confidence interval (c.i.) of at least 6 measurements of the same aliquot. See main text and Supplementary Information for details. bce = breccia, ilm = ilmenite; QNB = quartz-normative basalt, olv = olivine, pgt = pigeonite.

Identifying magmatic processes in lunar basalt sources. The average $\delta^{49}Ti$ values obtained for low- and high-Ti mare basalts (+0.010 ± 0.047 ‰ and +0.037 ± 0.071 ‰) are consistent with findings by Millet *et al.* (2016) and are indistinguishable from their Bulk Silicate Earth estimate (BSE: +0.005 ± 0.005 ‰, 95 % c.i.; see Fig. 1). The $\delta^{49}Ti$ value of our most primitive sample, the Apollo 12 olivine basalt

12004 (possibly tapping bulk lunar mantle) is identical with the $\delta^{49}Ti_{BSE}$ estimate by Millet *et al.* (2016) and the chondritic $\delta^{49}Ti$ value proposed by Greber *et al.* (2017b) but lower than the chondritic $\delta^{49}Ti$ value suggested by Deng *et al.* (2018b). Possible explanations for the observed intra-group $\delta^{49}Ti$ variations in mare basalts include fractional crystallisation of ilmenite during petrogenesis, assimilation of an IBC- or
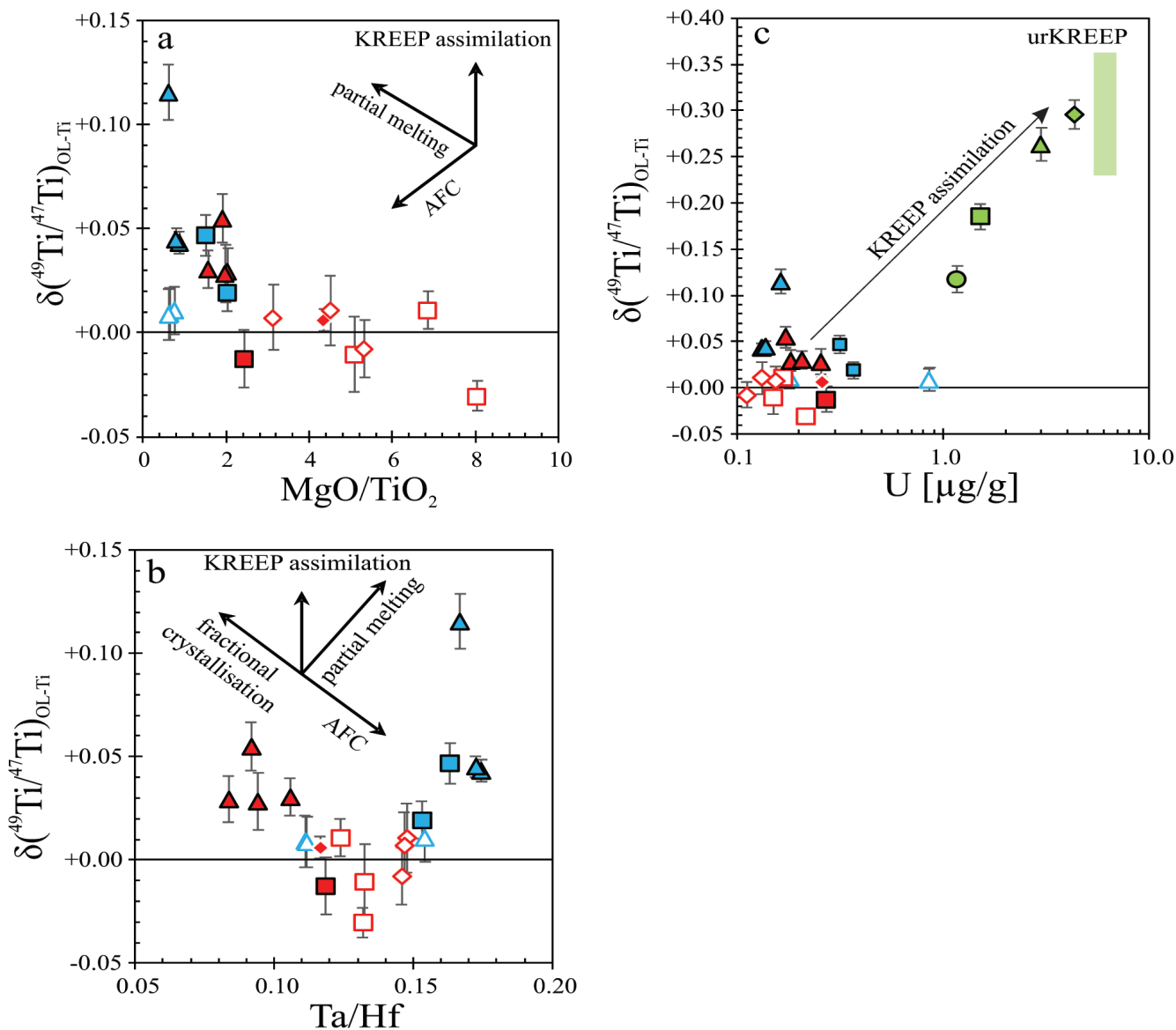
Figure 2 Plots of **(a)** δ^{49}Ti vs. MgO/TiO$_2$, **(b)** δ^{49}Ti vs. Ta/Hf and **(c)** δ^{49}Ti vs. U that can be used to discriminate between processes leading to variations in δ^{49}Ti. Symbols are the same as in Figure 1, black arrows indicate the direction in which a process would influence the values along y- and x-axes. Partial melting assumes the presence of ilmenite in the source, fractional crystallisation always implies fractional crystallisation of ilmenite. AFC implies the assimilation of an IBC component during ilmenite-free fractional crystallisation of a low-Ti magma. **(b)** The estimated Ta/Hf value of urKREEP is ~0.11 (Warren and Taylor, 2014). **(c)** Contamination by urKREEP (coloured arrow), would imply higher U contents (not observed). urKREEP is based on our first model (see Supplementary Information).

KREEP-component during fractional crystallisation, partial melting an IBC or mantle source heterogeneity. To distinguish between these processes we first consider the results of experimental studies that simulated the petrogenesis of lunar basalts (see Supplementary Information; Longhi, 1992 and references therein): For instance, experimentally synthesised low-Ti-like samples showed that ilmenite has been one of the first solidus phases (Longhi, 1992 and references therein), which would preferentially incorporate light Ti isotopes, increasing the δ^{49}Ti$_{melt}$ during fractional crystallisation of ilmenite (Millet *et al.*, 2016). High-Ti basalts from Apollo 17 were shown to originate from greater depths than Apollo 12 and 15 low-Ti mare basalts were successfully modelled by partial melting of an ilmenite-rich source (Longhi, 1992 and references therein). This can explain the observed elevated δ^{49}Ti$_{high-Ti}$ values (See Fig. 2a; Millet *et al.*, 2016). In contrast, the full assimilation of an IBC-component during fractional crystallisation of a low-Ti magma would decrease the δ^{49}Ti value of the basaltic melt (Fig. 2a). Thus, the small intra-group variations in δ^{49}Ti values

of low- and high-Ti basalts can best be explained by fractional crystallisation of ilmenite and melting of ilmenite-bearing sources, respectively.

In addition to experimental petrological studies, geochemical tools can help distinguish between the discussed processes. For example, the compatibility of HFSEs in ilmenite is variable (Münker, 2010): tantalum is the most compatible HFSE in ilmenite, whereas Hf is the most incompatible (*e.g.,* $D_{Ta} > 1 > D_{Hf}$; Leitzke *et al.*, 2016; or $D_{Ta} > D_{Hf}$, van Kan Parker *et al.*, 2011). Thus, fractional crystallisation of ilmenite would increase the δ^{49}Ti$_{melt}$ (Millet *et al.*, 2016) but decrease the Ta/Hf$_{melt}$ (Münker, 2010). In contrast, partial melting of an IBC component would increase the Ta/Hf$_{melt}$ and the δ^{49}Ti$_{melt}$ value ($D_{Ta} \sim 2 \times D_{Hf}$ for ilmenite, *e.g.,* Leitzke *et al.*, 2016). Apollo 12 low-Ti ilmenite basalts show lower Ta/Hf and positive δ^{49}Ti relative to the most primitive lunar basalt analysed in this study, (12004, see Figs. 1, 2b), indicating the early fractional crystallisation of ilmenite, which is consistent with

experimental results (Longhi, 1992 and references therein). Relatively low δ^{49}Ti values in Apollo 15 low-Ti basalts may indicate the assimilation of an IBC material (Longhi, 1992 and references therein). However, assimilation of an IBC component seems inconsistent with relatively low Ta/Hf and comparatively low TiO_2 contents of ~1.3 %. The assimilation of a KREEP-component would cause a substantial increase in the δ^{49}Ti and U concentration of the melt while barely fractionating Ta/Hf. Such trends are not observed indicating that KREEP components played an insignificant role during the petrogenesis of low- and high-Ti basalts (Fig. 2c). Apollo 17 high-Ti samples are rich in TiO_2, exhibit relatively low MgO/TiO_2 but high δ^{49}Ti and higher Ta/Hf relative to our most primitive sample. In agreement with the experimental evidence, this geochemical pattern strongly indicates partial melting of an IBC component during the petrogenesis of Apollo 17 high-Ti basalts (Longhi, 1992 and references therein). These processes are further modelled and discussed in the Supplementary Information.

Comparison with Fe isotope systematics. Previous studies observed a bimodal distribution of δ^{57}Fe values for lunar low-Ti and high-Ti basalts: higher δ^{57}Fe values in high-Ti basalts were attributed to the presence of ilmenite during partial melting (Sossi and Moynier, 2017; Sossi and O'Neill, 2017), which is consistent with experimental studies (Longhi, 1992 and references therein) as well as our Ta/Hf and δ^{49}Ti data. However, intra-group variation in δ^{57}Fe of low-Ti basalts was not observed (Weyer *et al.*, 2005; Sossi and Moynier, 2017; Poitrasson *et al.*, 2019) as the δ^{57}Fe of low-Ti basalts is mainly controlled by fractional crystallisation of olivine and pyroxene, which would preferentially incorporate light Fe isotopes, similar to ilmenite ($\Delta^{57}Fe_{Ilm-Ol}$ = +0.01 ‰; Sossi and O'Neill, 2017). Thus, δ^{49}Ti appear more appropriate to discriminate better between the petrogenetic processes culminating in lunar basalts. Additional Cr, V and Hf isotope systematics are discussed in the Supplementary Information.

Conclusion

New Ti isotope data for a representative set of lunar samples show that there is a clear offset between KREEP-rich samples and mare basalts, in agreement with previous work (Millet *et al.*, 2016; Greber *et al.*, 2017b). Our data reveal intra-group variation amongst olivine- and quartz-normative and (low-Ti) ilmenite mare basalts with the latter recording higher δ^{49}Ti than the former. High-Ti mare basalts have overall higher δ^{49}Ti. The δ^{49}Ti of our lunar sample suite, coupled with HFSE data, suggests that the fractional crystallisation of ilmenite and partial melting of an IBC-component are the principal processes affecting the δ^{49}Ti of Apollo 12 low-Ti mare basalts, and of Apollo 17 high-Ti mare basalts, respectively. This conclusion is consistent with results of previously published experimental studies (Longhi, 1992 and references therein). This is in excellent agreement with previous experimental data and the heavy δ^{57}Fe of high-Ti mare basalts (Longhi, 1992; Weyer *et al.*, 2005; Sossi and Moynier, 2017; Charlier *et al.*, 2018). Based on coupled HFSE and δ^{49}Ti data, the petrogenesis of high-Ti mare basalts by assimilation of IBC-component by low-Ti magma is unlikely.

Acknowledgements

Editor: Horst R. Marschall

Additional Information

References

ASPHAUG, E. (2014) Impact Origin of the Moon? *Annual Review of Earth and Planetary Sciences* 42, 551–578.

CHARLIER, B., GROVE, T.L., NAMUR, O., HOLTZ, F. (2018) Crystallization of the lunar magma ocean and the primordial mantle-crust differentiation of the Moon. *Geochimica et Cosmochimica Acta* 234, 50–69.

DENG, Z., CHAUSSIDON, M., SAVAGE, P., ROBERT, F., PIK, R., MOYNIER, F. (2019) Titanium isotopes as a tracer for the plume or island arc affinity of felsic rocks. *Proceedings of the National Academy of Sciences* 201809164.

DENG, Z., MOYNIER, F., SOSSI, P.A., CHAUSSIDON, M. (2018a) Bridging the depleted MORB mantle and the continental crust using titanium isotopes. *Geochemical Perspectives Letters* 9, 11–15.

DENG, Z., MOYNIER, F., VAN ZUILEN, K., SOSSI, P.A., PRINGLE, E.A., CHAUSSIDON, M. (2018b) Lack of resolvable titanium stable isotopic variations in bulk chondrites. *Geochimica et Cosmochimica Acta* 239, 409–419.

GREBER, N.D., DAUPHAS, N., BEKKER, A., PTÁČEK, M.P., BINDEMAN, I.N., HOFMANN, A. (2017a) Titanium isotopic evidence for felsic crust and plate tectonics 3.5 billion years ago. *Science* 357, 1271–1274.

GREBER, N.D., DAUPHAS, N., PUCHTEL, I.S., HOFMANN, B.A., ARNDT, N.T. (2017b) Titanium stable isotopic variations in chondrites, achondrites and lunar rocks. *Geochimica et Cosmochimica Acta* 213, 534–552.

GROSS, J., JOY, K.H. (2016) Evolution, Lunar: From Magma Ocean to Crust Formation. In: Cudnik, B. (Ed.) *Encyclopedia of Lunar Science.* Springer International Publishing, Cham, 1–20.

LEITZKE, F.P., FONSECA, R.O.C., MICHELY, L.T., SPRUNG, P., MÜNKER, C., HEUSER, A., BLANCHARD, H. (2016) The effect of titanium on the partitioning behavior of high-field strength elements between silicates, oxides and lunar basaltic melts with applications to the origin of mare basalts. *Chemical Geology* 440, 219–238.

LEITZKE, F.P., FONSECA, R.O.C., GÖTTLICHER, J., STEININGER, R., JAHN, S., PRESCHER, C., LAGOS, M. (2018) Ti K-edge XANES study on the coordination number and oxidation state of Titanium in pyroxene, olivine, armalcolite, ilmenite, and silicate glass during mare basalt petrogenesis. *Contributions to Mineralogy and Petrology* 173, 103.

Lin, Y., Tronche, E.J., Steenstra, E.S., van Westrenen, W. (2017) Experimental constraints on the solidification of a nominally dry lunar magma ocean. *Earth and Planetary Science Letters* 471, 104–116.

Longhi, J. (1992) Experimental petrology and petrogenesis of mare volcanics. *Geochimica et Cosmochimica Acta* 56, 2235–2251.

Mandl, M.B., Fehr, M.A., Schönbächler, M. (2018) Titanium stable isotope fractionation on the Moon: Evidence for inter- mineral isotopic fractionation. *Goldschmidt Abstracts* 2018 1666.

Millet, M.-A., Dauphas, N. (2014) Ultra-precise titanium stable isotope measurements by double-spike high resolution MC-ICP-MS. *Journal of Analytical Atomic Spectrometry* 29, 1444.

Millet, M.-A., Dauphas, N., Greber, N.D., Burton, K.W., Dale, C.W., Debret, B., Macpherson, C.G., Nowell, G.M., Williams, H.M. (2016) Titanium stable isotope investigation of magmatic processes on the Earth and Moon. *Earth and Planetary Science Letters* 449, 197–205.

Münker, C. (2010) A high field strength element perspective on early lunar differentiation. *Geochimica et Cosmochimica Acta* 74, 7340–7361.

Poitrasson, F., Zambardi, T., Magna, T., Neal, C.R. (2019) A reassessment of the iron isotope composition of the Moon and its implications for the accretion and differentiation of terrestrial planets. *Geochimica et Cosmochimica Acta* 267, 257–274.

Rapp, J.F., Draper, D.S. (2018) Fractional crystallization of the lunar magma ocean: Updating the dominant paradigm. *Meteoritics & Planetary Science* 53, 1432–1455.

Schauble, E.A. (2004) Applying Stable Isotope Fractionation Theory to New Systems. *Reviews in Mineralogy and Geochemistry* 55, 65–111.

Simon, S.B., Sutton, S.R. (2017) Valence of Ti, V, and Cr in Apollo 14 aluminous basalts 14053 and 14072. *Meteoritics & Planetary Science* 52, 2051–2066.

Snyder, G.A., Taylor, L.A., Neal, C.R. (1992) A chemical model for generating the sources of mare basalts: Combined equilibrium and fractional crystallization of the lunar magmasphere. *Geochimica et Cosmochimica Acta* 56, 3809–3823.

Sossi, P.A., Moynier, F. (2017) Chemical and isotopic kinship of iron in the Earth and Moon deduced from the lunar Mg-Suite. *Earth and Planetary Science Letters* 471, 125–135.

Sossi, P.A., O'Neill, H.St.C. (2017) The effect of bonding environment on iron isotope fractionation between minerals at high temperature. *Geochimica et Cosmochimica Acta* 196, 121–143.

Sprung, P., Kleine, T., Scherer, E.E. (2013) Isotopic evidence for chondritic Lu/Hf and Sm/Nd of the Moon. *Earth and Planetary Science Letters* 380, 77–87.

Thiemens, M.M., Sprung, P., Fonseca, R.O.C., Leitzke, F.P., Münker, C. (2019) Early Moon formation inferred from hafnium–tungsten systematics. *Nature Geoscience* 12, 696–700.

van Kan Parker, M., Mason, P.R.D., van Westrenen, W. (2011) Trace element partitioning between ilmenite, armalcolite and anhydrous silicate melt: Implications for the formation of lunar high-Ti mare basalts. *Geochimica et Cosmochimica Acta* 75, 4179–4193.

Warren, P.H., Taylor, G.J. (2014) The Moon. *Treatise on Geochemistry (Second Edition)* 2, 213–250.

Warren, P.H., Wasson, J.T. (1979) The origin of KREEP. *Reviews of Geophysics* 17, 73.

Weyer, S., Anbar, A., Brey, G., Munker, C., Mezger, K., Woodland, A. (2005) Iron isotope fractionation during planetary differentiation. *Earth and Planetary Science Letters* 240, 251–264.